HHS Public Access

Author manuscript

Science. Author manuscript; available in PMC 2016 March 27.

Published in final edited form as:

Science. 2013 March 1; 339(6123): 1077–1080. doi:10.1126/science.1233009.

Genomic analysis of non-*NF2* meningiomas reveals mutations in *TRAF7*, *KLF4*, *AKT1*, and *SMO*

Victoria E. Clark[1], **E. Zeynep Erson-Omay**[1], **Akdes Serin**[1], **Jun Yin**[2], **Justin Cotney**[2], **Koray Özduman**[3], **Timuçin Avşar**[4], **Jie Li**[5], **Phillip B. Murray**[1], **Octavian Henegariu**[1], **Saliha Yilmaz**[1], **Jennifer Moliterno Günel**[6], **Geneive Carrión-Grant**[1], **Baran Yılmaz**[7], **Conor Grady**[1], **Bahattin Tanrıkulu**[7], **Mehmet Bakırcıoğlu**[1], **Hande Kaymakçalan**[8], **Ahmet Okay Caglayan**[1], **Leman Sencar**[1], **Emre Ceyhun**[1], **A. Fatih Atik**[7], **Yaşar Bayri**[7], **Hanwen Bai**[1], **Luis E. Kolb**[1], **Ryan Hebert**[1], **S. Bulent Omay**[1], **Ketu Mishra-Gorur**[1], **Murim Choi**[2], **John D. Overton**[9], **Eric C. Holland**[10], **Shrikant Mane**[2,9], **Matthew W. State**[11], **Kaya Bilgüvar**[1], **Joachim M. Baehring**[12], **Philip H. Gutin**[6], **Joseph M. Piepmeier**[13], **Alexander Vortmeyer**[5], **Cameron W. Brennan**[14], **M. Necmettin Pamir**[3], **Türker Kılıç**[15], **Richard P. Lifton**[2,16], **James P. Noonan**[2,17], **Katsuhito Yasuno**[1], and **Murat Günel**[1,18,*]

1

2

3

4

5

6

7

8

9

10

11

12

13

14

15

16

[*]To whom correspondence should be addressed: murat.gunel@yale.edu.

Supplementary Materials
Materials and Methods
Figures S1–S14
Tables S1–S8
References (13–27)

17

18

Abstract

We report genomic analysis of 300 meningiomas, the most common primary brain tumors, leading to the discovery of mutations in *TRAF7*, a proapoptotic E3 ubiquitin ligase, in nearly one-fourth of all meningiomas. Mutations in *TRAF7*commonly occurred with a recurrent mutation (K409Q) in *KLF4*, a transcription factor known for its role in inducing pluripotency, or with $AKT1^{E17K}$, a mutation known to activate the PI3K pathway. *SMO* mutations, which activate Hedgehog signaling, were identified in ~5% of non-*NF2* mutant meningiomas. These non-*NF2* meningiomas were clinically distinctive—nearly always benign, with chromosomal stability, and originating from the medial skull base. In contrast, meningiomas with mutant *NF2* and/or chromosome 22 loss were more likely to be atypical, showing genomic instability, and localizing to the cerebral and cerebellar hemispheres. Collectively, these findings identify distinct meningioma subtypes, suggesting avenues for targeted therapeutics.

Meningiomas, arising from the meninges of the central nervous system, are the most common primary brain tumors, with a prevalence of ~170,000 cases in the United States (1). Although most are histologically classified as benign (grade I), about 10% represent atypical (grade II) or anaplastic (grade III) forms. Meningiomas frequently invade surrounding brain and critical neurovascular structures, often causing neurological deficits and requiring surgical intervention. Loss of *Neurofibromin 2* (*merlin, NF2*) is found in 40 to 60% of sporadic meningiomas (2), but the genetic architecture of the remainder remains obscure, limiting options for the development of rational therapies.

To comprehensively characterize the genomics of meningioma and to gain further insight into molecular mechanisms of tumor formation, we performed genome-wide genotyping and exome sequencing (average depth of coverage 255-fold) of 50 previously nonirradiated grade I (n = 39) and grade II (n = 11) meningiomas and matched normal DNA (3) (table S1). For the meningiomas in which matching blood samples were available (n = 39), the mean number of protein-altering somatic mutations was 7.2 (range 1 to 15), a considerably smaller number compared with malignant tumors (table S2). We next searched for genes with significantly more somatic mutations than expected by chance (fig. S1). Besides *NF2*, we identified increased mutation burden in *TNF receptor-associated factor* 7 (*TRAF7*), *Krupple-like factor 4* (*KLF4*), *v-akt murine thymoma viral oncogene homolog 1* (*AKT1*), and *Smoothened, frizzled family receptor* (*SMO*) (as a group, referred to as *non-NF2* mutant hereafter) (Fig. 1). Mutations in these genes were mutually exclusive of *NF2* mutations. In addition, we identified single mutations in genes previously reported to play a role in other neoplasias, including *CREBBP*, *PIK3CA* (R108H variant), *PIK3R1* (deletion p.306-307), and *BRCA1* as well as two *SMARCB1* mutations, which coexisted with *NF2* loss and have previously been reported in meningiomas (4) (table S3).

We next performed targeted resequencing of these top five genes, along with chromosome 22 copy-number analysis, in an independent set of 250 unradiated meningiomas (204 grade I and 46 high-grade meningiomas) (fig. S2). In the combined analysis of 300 meningiomas,

we identified coding mutations in one of these five genes and/or evidence for chromosome 22 loss in 237 (79%) (Fig. 2A and table S3). *NF2* mutations were present in 108 (36%). *TRAF7* mutations, which were always exclusive of *NF2* mutations [mutual exclusivity *P* value (P_{me}) = 2.55×10^{-17} (5)], were observed in nearly one-fourth of the meningiomas examined (n = 72). TRAF7 is a proapoptotic N-terminal RING and zinc finger domain protein with E3 ubiquitin ligase activity that contains seven WD40 repeats in its C terminus (6). TRAF7 interacts with several molecules, such as MEKK3, through these WD40 repeats, affects multiple signaling pathways, including NF-κB, and targets ubiquitination of proteins including c-FLIP, an antiapoptotic molecule (7). It is notable that 67 of the 72 TRAF7 mutations, including 15 recurrent mutations, all map to the WD40 domains (Fig. 2B).

In the transcription factor *KLF4*, we identified a recurrent K409Q mutation, which almost always co-occurred with *TRAF7* mutations [n = 31; co-occurrence *P* value (P_{co}) = 2.50×10^{-20}] and were exclusive of *NF2* mutations ($P_{me} = 3.77 \times 10^{-7}$). KLF4 is expressed in meningiomas (fig. S3). KLF4 regulates differentiation of several cell types and is best known as one of four genes that together promote reprogramming of differentiated somatic cells into pluripotent stem cells (8). Deletion of the KLF4 DNA binding domain blocks differentiation and induces self-renewal in hematopoietic cells (9). The recurrently mutated KLF4 residue, K409, lies within the first zinc finger and makes direct DNA contact in the major groove of the DNA binding motif (9) (Fig. 2C and fig. S4).

The known neoplasia-related recurrent mutation, $AKT1^{E17K}$, was identified in 38 meningiomas. Although the $AKT1^{E17K}$ mutation co-occurred with *TRAF7* mutations in 25 of the 38 tumors ($P_{co} = 3.90 \times 10^{-9}$), it was exclusive of the $KLF4^{K409Q}$ ($P_{me} = 1.18 \times 10^{-2}$) and *NF2* mutations, except in one case ($P_{me} = 2.70 \times 10^{-7}$). The $AKT1^{E17K}$ mutation has been shown to activate PI3K/AKT signaling (10) and was readily detectable by immunohistochemistry using an antibody specific for this mutation (fig. S3).

Finally, in 11 tumors, we identified mutations in *SMO*, which is expressed in meningiomas (fig. S5). These mutations include a recurrent L412F variant in seven meningiomas and a previously reported W535L mutation, which has been shown to result in activation of Hedgehog signaling in basal cell carcinoma (11). Eight of these SMO mutations were mutually exclusive of mutations in the other four genes ($P_{me} = 1.24 \times 10^{-2}$).

We next evaluated chromosomal instability. Chromosome 22 loss, observed in 149 tumors, was the most common event and was strongly associated with the presence of coding *NF2* mutations ($P_{co} = 1.32 \times 10^{-47}$). These were also significantly associated with higher grade meningiomas [$P = 5.90 \times 10^{-5}$; odds ratio (OR) = 3.54]. Higher-grade tumors also showed an increased number of large-scale chromosomal abnormalities (Fig. 2D and fig. S6) (6.9 versus 1.7 events per tumor) and an increased rate of *NF2* mutations (P = 0.03; OR = 1.96) and were observed more frequently in males than females ($P = 6.45 \times 10^{-4}$; OR = 2.93).

Given these observations pointing to distinct tumor subtypes based on mutation profiles, we examined whether the mutation spectrum correlated with anatomical distribution and histological subtype. We initially grouped cerebral meningiomas into those originating along the skull base or those present in the cerebral hemispheres (Fig. 2E, fig. S7, and table S4).

Interestingly, tumors with *NF2* mutations and/or chromosome 22 loss (*NF2/chr22loss*) were predominantly found in the hemispheres ($P = 9.22 \times 10^{-14}$; OR = 6.74) with nearly all posterior cerebral (parieto-occipital), cerebellar, or spinal meningiomas being *NF2/chr22loss* tumors (fig. S8). For the meningiomas originating from the skull base, we observed a difference between those originating from medial versus lateral regions. The vast majority of *non-NF2* meningiomas were medial ($P = 4.36 \times 10^{-8}$; medial versus lateral OR = 8.80), whereas the lateral and posterior skull base meningiomas had *NF2/chr22loss* ($P = 1.55 \times 10^{-12}$; OR = 23.11). Meningiomas with only the recurrent *SMO* L412F mutation ($n = 5$) all localized to the medial anterior skull base, near the midline. This is particularly interesting because mutations in Hedgehog signaling result in holoprosencephaly, the midline failure of embryonic forebrain to divide into two hemispheres (12).

Mutational profiles also were correlated with histological diagnoses. For example, all of the meningiomas with a “secretory” component ($n = 12$), which follow a more aggressive clinical course owing to increased brain swelling, carried both *TRAF7* and*KLF4* mutations ($P_{co} = 6.02 \times 10^{-12}$) (fig. S9).

Consistent with these clinical observations, unsupervised hierarchical clustering of meningiomas based on gene expression and chromatin immunoprecipitation for H3K27 acetylation followed by sequencing (H3K27ac ChIP-seq) analyses confirmed clustering into *NF2/chr22loss* versus *non-NF2* mutant subgroups (Fig. 2F and figs. S10 and S11) and revealed several molecules whose acetylation and expression was specific to a subtype (tables S5 and S6). For these differentially expressed genes, there was a strong correlation between expression and ChIP-seq data (fig. S12). Among the *non-NF2* meningiomas, *SMO* mutants were clearly defined by increased expression and activation of the Hedgehog pathway (fig. S13 and tables S7 and S8).

These results clearly identify meningioma subgroups, distinguishing them based on their mutually exclusive distribution of mutations, distinct potential for chromosomal instability and malignancy, anatomical location, histological appearance, gene expression, and H3K27ac profile. Our results show that the mutational profile of a meningioma can largely be predicted based on its anatomical position, which in turn may predict likely drug response (e.g., Hedgehog inhibitors for midline tumors). This may prove relevant for surgically unresectable, recurrent, or invasive meningiomas and could spare patients surgery or irradiation, an independent risk factor for progression of these generally benign tumors.

Supplementary Material

Refer to Web version on PubMed Central for supplementary material.

Acknowledgments

We are grateful to the patients and their families who have contributed to this study. This study was supported by the Gregory M. Kiez and Mehmet Kutman Foundation. R.P.L. is an investigator of the Howard Hughes Institute. V.E.C. is supported by NIH T32GM07205. All somatic mutations identified through exome sequencing of meningiomas are reported in the supplementary materials and submitted to the Catalogue of Somatic Mutations in Cancer (COSMIC) database (http://cancer.sanger.ac.uk/cancergenome/projects/cosmic, submission ID COSP30702). Yale University has filed a provisional patent application based on the results of this study.

References and Notes

1. Wiemels J, Wrensch M, Claus EB. J Neurooncol. 2010; 99:307. [PubMed: 20821343]
2. Riemenschneider MJ, Perry A, Reifenberger G. Lancet Neurology. 2006; 5:1045. [PubMed: 17110285]
3.
Materials and methods are available as supporting material on Science online.
4. Schmitz U, et al. Br J Cancer. 2001; 84:199. [PubMed: 11161377]
5. Cui Q. PloS One. 2010; 5
6. Xu LG, Li LY, Shu HB. J Biol Chem. 2004; 279:17278. [PubMed: 15001576]
7. Bouwmeester T, et al. Nat Cell Biol. 2004; 6:97. [PubMed: 14743216]
8. Takahashi K, et al. Cell. 2007; 131:861. [PubMed: 18035408]
9. Schuetz A, et al. Cell Mol Life Sci. 2011; 68:3121. [PubMed: 21290164]
10. Carpten JD, et al. Nature. 2007; 448:439. [PubMed: 17611497]
11. Xie J, et al. Nature. 1998; 391:90. [PubMed: 9422511]
12. Roessler E, et al. Nature Genetics. 1996; 14:357. [PubMed: 8896572]

Tumor	Grade	Chr22 loss	NF2	TRAF7	AKT1	KLF4	SMO
MN-95	1	Yes					
MN-290	1	Yes					
MN-1041	1	Yes					
MN-1047	1	Yes					
MN-1137	1	Yes					
MN-47	1	Yes	p.Q453X				
MN-52	1	Yes	p.F256fs				
MN-71	1	Yes	p.T59fs				
MN-81	1	Yes	p.Q65fs				
MN-169	1	Yes	p.E460X				
MN-288	1	Yes	p.K17_M29del				
MN-291	1	Yes	p.I210fs				
MN-293	1	Yes	p.Q459X				
MN-294	1	Yes	c.363+1G>C				
MN-297	1	Yes	p.K99fs				
MN-301	1	Yes	p.W41fs				
MN-306	1	Yes	p.K44X				
MN-1091	1	Yes	p.L14fs				
MN-1133	1	Yes	p.Y207fs				
MN-26	1			p.C388Y	p.E17K		
MN-105	1			p.R641C	p.E17K		
MN-292	1			p.Q637H	p.E17K		
MN-191	1			p.K615E		p.K409Q	
MN-201	1			p.L580del		p.K409Q	
MN-249	1			p.R641C		p.K409Q	
MN-1025	1			p.G536S		p.K409Q	
MN-1066	1			p.N520S		p.K409Q	
MN-303	1			p.S561N			
MN-206	1			p.G390E			
MN-304	1			p.R653Q			
MN-305	1			p.G536S			
MN-1053	1			p.E353insFRRDAS			
MN-1045	1						p.L412F
MN-1132	1						p.W535L
MN-164	2	Yes					
MN-22	2	Yes	c.115-1G>A				
MN-54	2	Yes	p.Q319X				
MN-96	2	Yes	p.L14fs				
MN-97	2	Yes	p.M426fs				
MN-171	2	Yes	p.L208P				
MN-295	2	Yes	p.E103fs				
MN-298	2	Yes	p.V24fs				
MN-1054	2	Yes	p.R262X				
MN-16	2	Yes		p.T145M	p.E17K		
MN-1144	2	Yes		p.F337S			

Fig. 1.

Exome sequencing identifies meningioma subgroups based on mutually exclusive mutation profiles.

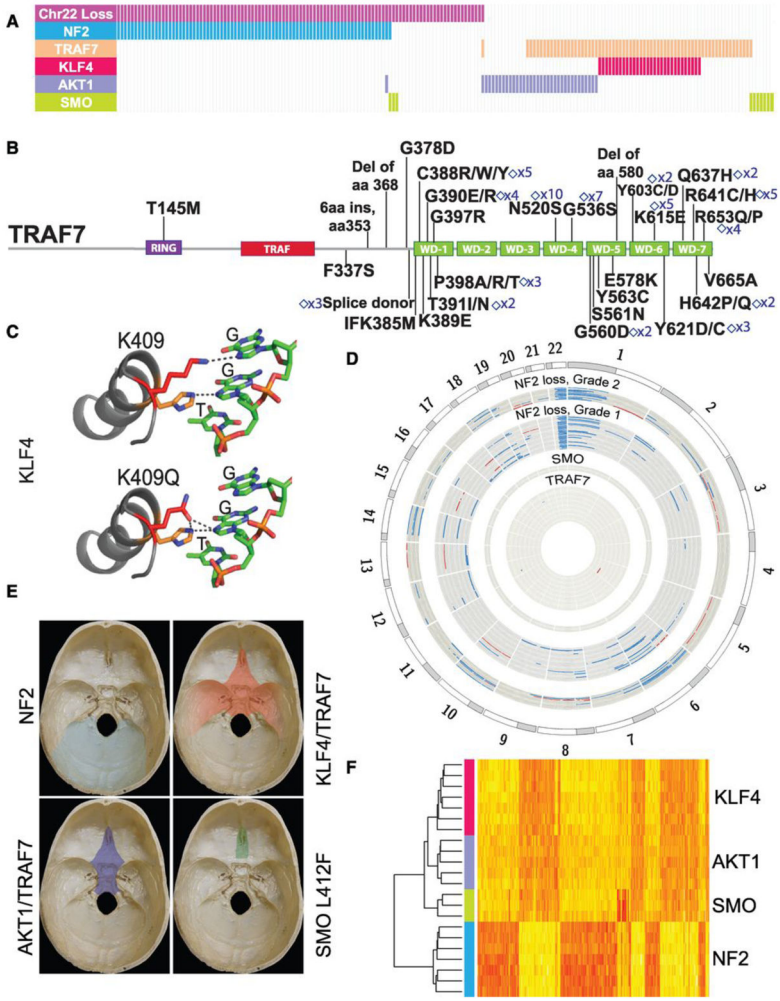

Fig. 2.

Genomic architecture of meningiomas. (**A**) *NF2*, *TRAF7*, and *SMO* coding mutations along with recurrent *AKT1*^{E17K} and *KLF4*^{K409Q} variants reveal meningioma subtypes with mutually exclusive profiles. Analysis for chromosome 22 copy number is also shown. Each bar represents a grade I meningioma sample; 191 samples are depicted. (**B**) *TRAF7* mutations, which are identified in 72 of 300 meningiomas analyzed, are clustered within its WD40 domains. The count of recurrent mutations, which are denoted by diamonds, is indicated. (**C**) The recurrent *KLF4*^{K409Q} mutation is located within the first zinc finger domain, which makes direct DNA contact. (**D**) Circos plot of large-scale genomic abnormalities identified (blue: deletion, red: amplification). Whereas all *NF2*/*chr22loss* meningiomas (outer circles, n = 41, including n = 30 with coding *NF2* mutations) show chromosome 22 loss, which is typically associated with further chromosomal abnormalities in grade II tumors (n = 11, including n = 8 with coding *NF2* mutations), genomic stability is a hallmark of grade I *non-NF2* tumors (inner circles, n = 36). (**E**) Along the skull base, *NF2/chr22loss* meningiomas originate from the lateral and posterior regions, whereas the vast majority of anterior and medial meningiomas are *non-NF2* mutant. (**F**) Unsupervised hierarchical clustering of gene expression profiles defines two major benign meningioma

subgroups, those with *NF2/chr22loss* and *non-NF2* mutant tumors. Each subgroup reveals differential H3K27ac and gene expression profiles (figs. S10 to S14 and tables S5 to S8).